

Field and Laboratory Investigations to Examine the Damage Category of Monumental Sandstone in Arid Regions: Seti I Temple, Upper Egypt; a Case Study

G. M. E. Kamh¹ and R. Azzam²

¹Geology Dept., Fac. of Science, Menoufiya University, Egypt (g_kamh2000@yahoo.com)

²Geology and Hydrogeology, LIH, RWTH, Aachen University, Germany

Abstract

Weathering acts with different intensities and rates on natural and artificial stones based on the dominant environmental conditions at a given area on one hand, limits of geotechnical parameters and durability of a given rock on the other hand. Recently, the environmental conditions became aggressive resulting in a severe damage to one of the most valuable and economic sectors at any country “the archaeological sites with its engravings and paintings”. El-Silsila sandstone is the most commonly used rock for building (in the past) and restoration (recently) of many archaeological sites in Egypt.

This paper aims to determine damage category of construction sandstone at arid regions taking Seti I Temple at Qurna “Upper Egypt” that had been built from the Upper Cretaceous sandstone of El-Silsila quarries as a case study; also, it aims to find out if a detailed field investigations, measuring dimensions of all weathering forms and field data processing using linear and progressive damage indices equations can in a semi-quantitative form verify the same damage category that can be quantitatively determined using a detailed laboratory analyses or not. Detailed measurements of weathering forms’ dimensions had been conducted and processed graphically and mathematically. Laboratory analyses including petrographic investigation, hydrochemical analysis and geotechnical investigations had been conducted for the rock samples collected from the study area. Both of field and laboratory investigations revealed that Seti I Temple has severe to very severe damage category as a whole site, also it revealed that salt weathering severely affect on the lower courses of this site. In addition, it has been proved that detailed field study and its data processing can to a great extent replace the laboratory investigations that require rock sampling that might be im-permissible at some cases.

Keywords: Sandstone, salt weathering, arid regions, Egypt, Seti I Temple

Untersuchungen vor Ort und im Labor, um die Kategorie der Schädigung von Sandstein im Wüstenklima festzustellen: Seti I Tempel, Oberägypten; eine Fallstudie

Zusammenfassung

Die Intensität und die Geschwindigkeit der Verwitterung von natürlichen und künstlich hergestellten Steinen hängt einerseits von den vorherrschenden klimatischen Bedingungen an einem gegebenen Ort ab und andererseits von Grenzwerten der geotechnischen Eigenschaften und der Beständigkeit eines vorliegenden Steins. In jüngster Zeit wurden die Umweltbedingungen aggressiver. Das führt zu erheblichen Schäden auf einem besonders wertvollen und auch ökonomisch bedeutenden Gebiet, nämlich die archäologischen Stätten mit ihren Skulpturen und Malereien. El-Silsila Sandstein ist der am häufigsten verwendete Naturstein für den Bau (in der Vergangenheit) und das Instandsetzen von vielen archäologischen Stätten in Ägypten.

In diesem Beitrag soll die Kategorie der Schädigung von Sandstein im Bauwesen in trockenem Klima als Fallstudie am Beispiel des Seti I Tempels in Qurna, in Oberägypten, behandelt werden. Dieser Sandstein kommt vom oberen cretazischen Sandstein der El-Silsila Steinbrüche. Gleichzeitig soll mit diesem Beitrag festgestellt werden, ob mit einer detaillierten Untersuchung vor Ort, bei der das Ausmaß jeder Form der Verwitterung sowie die Auswertung der Messwerte mit Hilfe von linearen und progressiven Schadensindices herangezogen werden, halbquantitativ dieselbe Schadenskategorie bestätigt werden kann, die man aufgrund von Laboruntersuchungen quantitativ bestimmt hat. Ins Einzelne gehende Messungen des Ausmaßes der Verwitterungsformen wurden durchgeführt and graphisch sowie mathematisch ausgewertet. Analysen im Labor wie etwa petrographische Bestimmungen, hydrochemische Analyse und geotechnische Untersuchungen wurden an Steinproben von der zu untersuchenden Stelle durchgeführt. Die Untersuchungen vor Ort sowie die Analysen im Labor erbrachten dasselbe Resultat, die gesamte Grabungsstätte des Seti I Tempels fällt in die Kategorie starke bis sehr starke Schädigung. Es stellte sich außerdem heraus, dass insbesondere die tiefer liegenden Teile der Stätte von Salzsäuren betroffen sind. Schließlich konnte festgestellt werden, dass Felduntersuchungen und deren Auswertung Laboruntersuchungen zu denen Probenentnahmen notwendig sind, die aber in einigen Fällen nicht vertretbar erscheinen, weitgehend ersetzt werden können.

Stichwörter: Sandstein, Salzverwitterung, Wüstenklima, Ägypten, Seti I Tempel.

1 Introduction

Weathering processes act worldwide at all climatic conditions and environments attacking sub-aerial natural and artificial building materials (stones, bricks, concreteetc). The duration, number of cycles and intensity of weathering processes are controlled by the major and minor changes in the environmental parameters (particularly air temperature and its relative humidity) at a given area as well as materials' physical, mechanical and durability limits. Previous literatures have been published in examining weathering processes, intensity, mechanisms and rate on natural and artificial building stones [1- 9].

It has been noted that weathering processes and intensity have been varied during the last few decades due to the major interference of human being in the environment resulting in raising concentration of all pollutants' types (air and water pollution, sound pollution, radial pollutionetc) [10-13]. It is in turn reflected passively on human life as well as construction rocks of valuable archaeological sites to an unlimited extent of damage [11-13].

The Seti I temple is one of the few remaining royal monuments that still intact at Abydos. It has been constructed in a valley opposite to Luxor City (Fig. 1 a). Seti I was the father of perhaps Egypt's greater rulers, Ramesses II. He ruled Egypt for 13 years i.e. from 1291 through 1278 BC (about

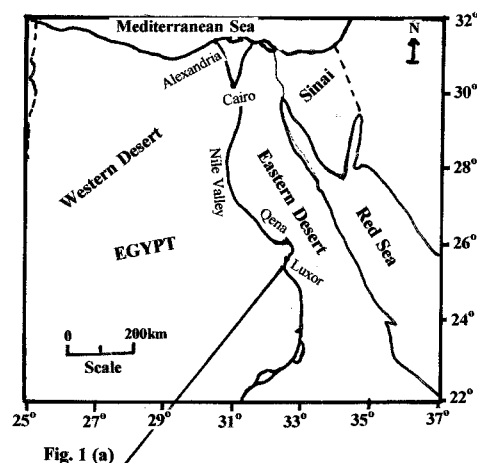


Fig. 1 (a)

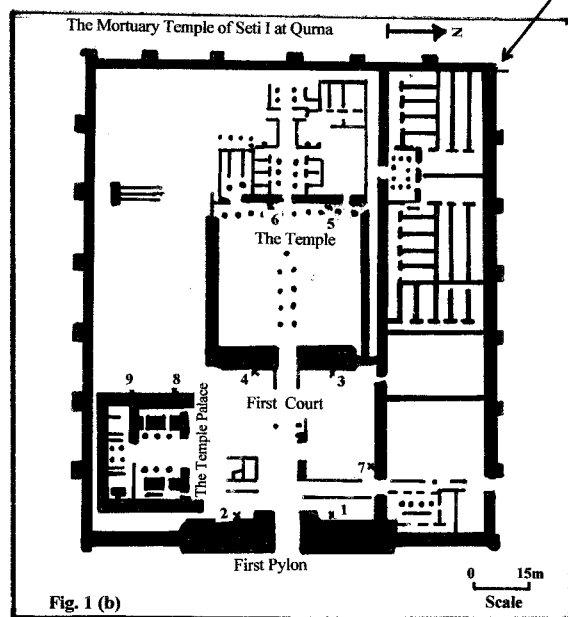


Fig. 1 (b)

Figure 1: Base map of Egypt presenting location of Seti I Temple (a); and sketch diagram of the Mortuary Temple of Seti I at Qurna with location of the collected rock samples (b).

3291 years BP). He started many projects e.g. the great Hypostyle Hall in the Temple of Amun at Karnak which his son Ramesses II later finished. At Abydos, he built perhaps the most remarkable temple ever constructed in Egypt. His tomb in the valley of Kings is one of the finest and deepest tombs in this valley. Seti I died before this temple was completed and his son Ramesses II completed it. It was as many pharaonic archaeological sites covered by sand in the valley of Kings. In the beginning of 18th Century (from 1816 – 1817 AC) Giovanni Belzoni was the first to dig in the Valley of Kings and discovered the tomb of Seti I. Later on, in the late of 19th Century, the tombs' of Amenhetep II and Tutankhamen were discovered.

Pilot studies have been conducted on pharaonic monuments in the western bank of the Nile e.g. Abydos, Temple of Dendara, Medinet Habu Temple at Qurna, ruin of Merenpetah at Qurna and Hatshepsut Temple in Dier El-Bahari as well as on the eastern bank e.g. Karnak Temple. It was mainly concerned with history or description of weathering features and weathering processes to be expected [8, 14, 15].

The current study aims to quantify damage category on the natural sandstone used for construction at such arid regions using detailed field investigation (including measuring dimensions of weathering forms to be presented graphically and mathematically using linear and progressive damage indices and the damage category scale of [16], and laboratory study for rock's texture and recession in its limits of geotechnical parameters compared with its un-weathered sandstone of El-Silsila quarries that had been tested before [17].

2 Geology and Environmental Conditions at the Study Area

The bedrock on which a given archaeological site is erected or through which an excavation has been carried out may have an impact on such site due to its un-stability [18, 19]. The geology and topography at a given area control wind direction, air heat flow towards or far-away the area ...etc and thus affect the environmental parameters to an extent. Also, the geology at a given area might throw light on the source rock used for building or restoration of the archaeological site at such area. In general, it is of value to mention the local geology at Seti I Temple and its surroundings.

The stratigraphic columnar section of Gebel Qurna opposite to Luxor is composed of two formations [20], namely; Esna Shale (55 m of shale with abundant limonitic fossils becoming marly) of late Paleocene-early Eocene (Yepresian), overlaid by Thebes Formation (345m thick of limestone and marl of variable composition, Fig. 2). Thebes Formation is composed of two members aligned from base to top: Hamidat Member and Dabbabia Member.

The study area is characterized by annual mean monthly temperature 25.6 °C with maximum mean in Summer 32.7 °C and minimum mean in Winter 17.3 °C. The maximum mean monthly temperature is 42 °C (in July) and its minimum mean is 9.6 °C (in January) [18]. The annual mean relative humidity is 37 %, the rainfall is limited and scarce with an average 4 – 7 cm/y [15]. So, the study area is considered as an arid to extremely arid at such limits of climatic parameters [18, 21].

3 Methodology

To achieve the aims of the current study, site investigation including field description and graphical documentation of weathering features at different parts of this temple has been carried out. Using Linear Damage index “ DI_{lin} ” and Progressive Damage index “ DI_{prog} ” equations listed below [16], we can achieve the overall damage category for each part under investigation at this temple considering area percentage of each damage category at each part. Then, the overall damage category of the whole site can be computed as an average value of damage indices at the examined areas. It must be known that the damage categories have been divided into six classes namely; category zero where no visible damage is recorded; category 1 where very slight damage is recorded; category 2 where slight damage is recorded; category 3 where medium damage is recorded; category 4 where severe damage is recorded; category 5 where very severe damage is recorded [16]. The damage severity of a given building (particularly construction rock with its paints and/or engravings) is defined by the historical importance of the building e.g. up to 0.5 cm damage in depth of pharaonic engravings can be considered as damage category 4 or 5, meanwhile, it is category 1 for historical stones with no engravings as huge size blocks constituting the Giza Pyramids [16].

Time units	Rock units		Lithologic column	Description and Thickness
	Formation	Member		
Early Eocene (Ypresian)	Thebes Formation	Dahababia Member	30 m. Yellow silicified limestone	30 m. Yellow silicified limestone
			30 m. Nummullitic limestone	30 m. Nummullitic limestone
			35 m. Limestone	35 m. Limestone
		Hamidat Member	75 m. Marl with scattered flint and pelecypods	75 m. Marl with scattered flint and pelecypods
120 m. Limestone with flint concretions	120 m. Limestone with flint concretions			
Late Paleocene	Esna Shale	55 m. shale with abundant limonitic fossils becoming marly	55 m. shale with abundant limonitic fossils becoming marly	

Figure 2: Stratigraphic columnar section of Gebel Qurna, opposite to Luxor, Upper Egypt (Said, 1990)

$$DI_{lin} = \{(A * 0) + (B * 1) + (C * 2) + (D * 3) + (E * 4) + (F * 5)\} / 100$$

$$= \{B + (C * 2) + (D * 3) + (E * 4) + (F * 5)\} / 100$$

$$DI_{prog} = \sqrt{\{(A * 0^2) + (B * 1^2) + (C * 2^2) + (D * 3^2) + (E * 4^2) + (F * 5^2)\} / 100}$$

$$= \sqrt{\{B + (C * 4) + (D * 9) + (E * 16) + (F * 25)\} / 100}$$

Where

A = area (%) – damage category 0

B = area (%) – damage category 1

C = area (%) – damage category 2

D = area (%) – damage category 3

E = area (%) – damage category 4

F = area (%) – damage category 5 and $\sum_A^F = 100$

The difference between (DI_{lin}) and (DI_{prog}) is increased as proportion of higher damage categories are increased i.e. $DI_{prog} \geq DI_{lin}$ [16].

Specimens have been collected from the severely weathered as well as slightly weathered parts of this temple. It has been petrographically examined through thin sections and Scanning Electron Microscope (Hitachi 3170S). This is to detect any damage of rock's texture on micro-scale and to be compared with the four types of El-Silsila sandstone quarries [17] that are expected to be the main source of con-

struction rock to Seti I Temple as well as other archaeological sites in Upper Egypt. Geotechnical parameters have been measured for each of un-weathered, slightly weathered and severely weathered sandstone using magneto-structive ultrasonic as a non-destructive technique, and as an alternative to time consuming destructive tools [22]. The geotechnical parameters to be examined for the collected rock samples are namely; velocity of ultrasonic waves "Cp" measured at both directions (parallel to and at right angle to lamination or bedding); and rock's internal friction "Qc". The examined sandstone samples have been prepared as rods of rectangulars with dimensions 32 x 8 x 6 mm following the method of [23]. The samples were excited by magneto-structive waves which are transformed to ultrasonic waves in a magnetic field. Then we record the frequency "f" of the waves and the initial wave intensity "A₀" as well as the steady wave intensity "A_t". Then, these parameters (Cp and Qc) have been computed from the following equations:

$$[(A_0 + A_t) / (A_0 - A_t)] = X$$

$$(\pi n / Qc) = \{\ln [2 / (1 - X)]\} / (1 + X)$$

$$Cp = 2 Lf / n$$

where L is the length of the examined rock sample "cm", the echo-form as well as equipment pattern is clear in figure 3.

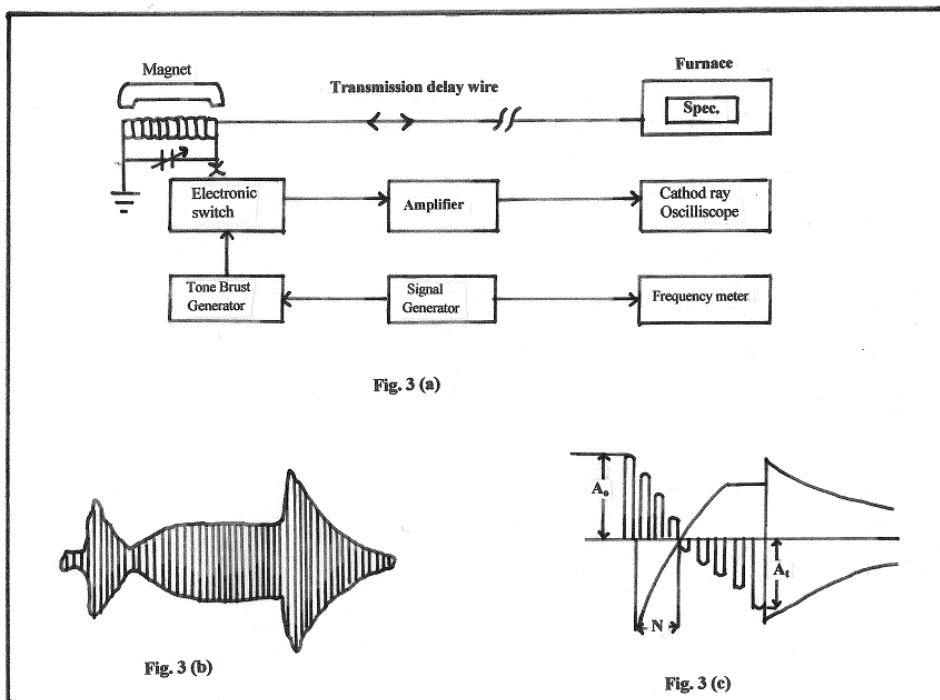


Figure 3: A magneto-structive system (a) schematic diagram of the magneto-structive Delay-line system, (b) Ideal Echo-form at a given mode number and (c) Schematic diagram of the resultant Echo-pattern Display in the Magneto-structive Delay-line system (after Kapranos et al., 1981)

Table 1: Weathering forms and its dimensions at some parts of Seti I Temple, "abbreviations of weathering forms based on Fitzner et al., 2002)

Part of investigation	Wall side orientation and points of concern	Weathering forms and its dimensions														
		Loss of stone material G1							Discoloration G2			Granular disintegration G3		Fissures G4		
		Wo (AV.)		Rh (AV.)	aO (AV.)		bO (AV.)	Ee area (%)	hkc			Gs (kg/m ²) (AV.)	tL (AV.)			
		Depth (cm)	Area (%)	depth (cm)	Depth (cm)	Covering area (%)	cm ³ /m ²		L.	M.	H.		Length (cm)	Width (cm)	Density/m ²	
First Pylon	West facing wall side	1	1,5	75	2,5	zero	zero	5100	80		M.		10,1	80	2	M.
		2	1,8	90	2,8	zero	zero	6400	93		M.	H.		10,9	73	1,5
First Court	East facing wall side	3	2,5	70	3,1	zero	zero	9546	65		M.		28,8	40	2,1	M.
		4	2,1	83	3,5	zero	zero	10118	73		M.		33	46	2	M.
The Temple	East facing wall side	5	3,1	80	3,1	2,7	8	20000	25	L.			36	40	0,5	L.
		6	2,2	72	2,5	3,8	11	18650	20	L.			33,6	50	0,6	L.
First Court	South facing wall side	7	1,3	53	zero	1,2	2,5	10000	60		M.		18	45	0,9	M.
The Temple Palace	West facing wall side	8	0,6	30	zero	3,1	25	800	7	L.			1,4	30	0,5	V.L.
		9	0,75	45	zero	2,8	20	1050	11	L.			1,8	zero	zero	Zero

Wo is Obliteration of ingraves (cm depth, % as covering area/m²)
 Rh is clearing out stone components (depth in cm)
 aO is break out due to anthropogenic impact (depth in cm and area %)
 bO is break out due to construction cause (cm³/m²)
 Ee is salt efflorescence (area %)
 hkc is light-colored crust tracing stone surface (L.- M.- H.)
 Gs is granular disintegration into sand (mass in gm)
 tL is fissures dependent on stone structure (length, width, density)
 AV is average value of the measuring unit of each weathering form

Hydrochemical analysis has been conducted for the extracted solutions prepared from the collected rock samples (following the method of [24]), using Ion Chromatograph at Aachen University. This is to get total dissolved salts (T.D.S.) and salts' type as

well as its percentage for the collected samples, and this can reflect the role and impact of salts on such construction rock at this arid region.

4 Results

The results include a detailed field investigation for weathering forms reported and measured at some parts of Seti I Temple as well as laboratory analyses for texture, micro-weathering features, rock salt content and limits of rock's geotechnical properties.

4.1 Field Study

The Mortuary Temple of Seti I at Qurna is a huge structure of rectangular shape, its geometry and internal structure can be noted on the sketch diagram (Fig. 1 b). It is mainly built from sandstone blocks of average dimensions 120 x 80 x 60 cm. It has about 24 columns in the temple in addition to other columns in the first and second pylons as well as the temple palace. Most of these blocks have engravings of the Seti I and his son Ramesses II life. The present day situation of these sandstone blocks is worth to be reported particularly the blocks close to and in contact with temple's floor (basal courses). The temple is surrounded by small cultivated areas and some primitive houses that certainly have no sewage water system but directly inject in the sub-soil layer reaching this temple. Large area of the temple's floor is severely damp while dry parts of it has thin solid crust of salts that attack the basal courses of this temple (Figs. 4 and 5). Other parts of this temple that are not severely attacked by salts also have weathering features as obliteration of engravings at heights up to 6 m above ground surface (Figs. 6 and 7). Some areas (including one or two parts) have been selected for damage category investigation at Seti I Temple, these parts have all weathering forms and damage intensities of this temple. The weathering forms and their dimensions at these parts of Seti I Temple (using weathering form scheme and abbreviations of [16]) are listed in table 1. Also, the intensities of characteristic weathering forms at the selected parts of Seti I Temple have been classified and presented in figure 8. A correlation scheme between weathering forms and damage categories has been created (Fig. 9) using damage category scale of [16].

These field investigations and its graphical presentations resulted in the computation of the Linear and Progressive damage intensities (DI_{lin} and DI_{prog} respectively) at each investigation part of Seti I Temple for each individual weathering form through the temple (Table 2). Then, the overall average damage for each weathering form through the whole temple has been computed (Table 2) to give the present damage category. For the determi-

nation of damage category for the whole temple considering all groups of weathering forms, the DCAW scheme of [16] has been used (Fig. 10) indicating that Seti I Temple has damage category 5 (very severe damage category). This is a quantitative to semi-quantitative determination of the damage category for Seti I Temple using field study and its data processing.

4.2 Laboratory Analyses

The laboratory analyses have been based on examining the petrography, limits of geotechnical parameters and salt content of each of the slightly and the severely weathered sandstone samples collected from Seti I Temple. This is compared with same analyses conducted for fresh (un-weathered El-Silsila sandstone) samples previously examined [17], to quantify the damage category. Furthermore, the laboratory results are also compared with the semi-quantitative damage category determined for this temple based on field investigations.

4.2.1 Petrographic Study

It has been conducted for the sandstone samples collected from Seti I Temple using a transmitting polarizing microscope. It revealed that this sandstone has arenite texture of quartz arenite to arkose in composition. It is light brown spotted sandstone as noted at the study area and it is very similar and highly matching sandstone type 1 of Gebel El-Silsila. The sandstone blocks in this temple are heterogeneous regarding grain size as examined and measured by a graticule eye-piece at the same magnification power using a transmitting polarizing microscope. One type has quartz grains moderately sorted, sub-rounded to sub-angular with an average grain size of 0.25 mm (i.e. medium size sandstone), mostly with point contacts and few with grain contacts. Silica overgrowth can hardly be noted on some quartz grains. Its average pore size is 0.18 mm, mostly as inter-connected pores of irregular shape involving brown color spots of iron oxide (Fig. 11). The other type of sandstone constituting Seti I Temple has also arenite texture, its quartz grains have an average grain size of 0.11mm i.e. fine grained sandstone, moderately to well sorted, point grain contacts dominates, noticeable porosity with concentric to irregular shape pores having an average diameter of 0.07 mm involving dark brown iron oxide spots (Fig. 12).

For more details on rock's texture, scanning electron microscopic investigation has been conducted for both sandstone types. It revealed that the medium size arenite sandstone, consists of euhedral



Figure 4: Severely weathered sandstone basal courses at West facing wall side of the first pylon (parts of investigation numbers 1 and 2), Seti I Temple.

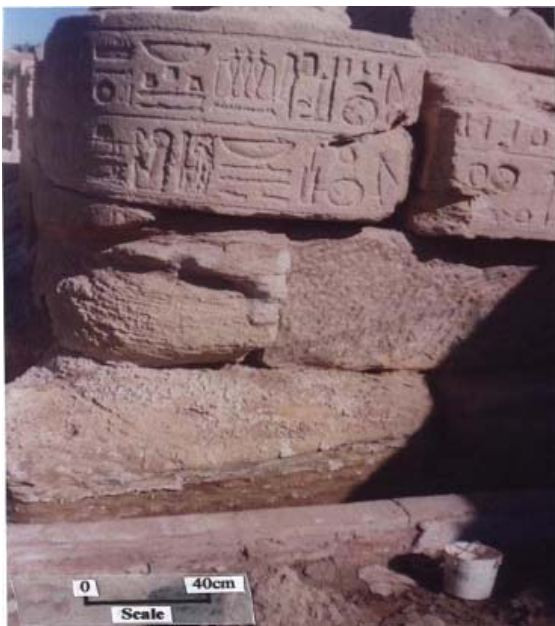


Figure 5: Severely weathered and damp sandstone basal courses at East facing wall side of the First Court (parts of investigation numbers 3 and 4), Seti I Temple.

quartz grains with silica overgrowth. Pitting and deformation of silica overgrowth can be traced and tiny size spherical shaped iron oxide particles that partially fill rock's pores, kaolinite can easily be traced (Fig. 13). At some parts, halite has been



Figure 6: Moderately weathered East facing wall side of the Temple (parts of investigation numbers 5 and 6).

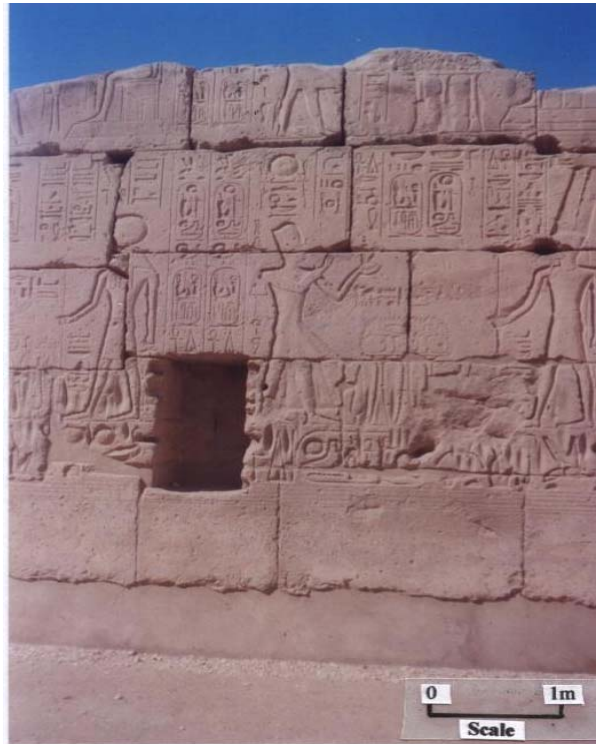


Figure 7: Slight to moderately weathered west facing wall side of the Seti I Temple, parts of investigation number 8 and 9.

detected (using SEM supported with EDX) covering most of the rock components (Fig. 14).

The fine grained sandstone has elongated euhedral quartz with silica overgrowth that scales off. Fragmentation and tiny pits can be noted on rock's quartz grains, kaolinite is easily detected as well as iron oxide spheres that partially fill most of the rock's pores

Group	Main weathering forms	Individual weathering forms	Classification of intensities	PART OF INVESTIGATION																		
				First Pylon		First Court		The Temple		First Court	The Temple Palace											
				West facing wall side		East facing wall side		East facing wall side		South facing wall side	West facing wall side											
				Point 1	Point 2	Point 3	Point 4	Point 5	Point 6	Point 7	Point 8	Point 9										
1- Loss of stone material (LS)	Back weathering (W)	Obliteration of ingravates (Wo)	Depth of Wo (cm) Intensity 1 < 0.5 Intensity 2 0.5 - 0.8 Intensity 3 0.8 - 1.3 Intensity 4 1.3 - 2.0 Intensity 5 > 2.0	1																		
				2																		
				3																		
				4																		
				5																		
			Area % of total Wo Intensity 1 < 5 Intensity 2 5 - 20 Intensity 3 20 - 25 Intensity 4 25 - 40 Intensity 5 > 40	1																		
				2																		
				3																		
				4																		
				5																		
	Relief (R.)	Clearing out of stone components (Rh)	Depth of Rh in (cm) Intensity 1 < 1.5 Intensity 2 1.5 - 2.5 Intensity 3 > 2.5	1																		
				2																		
				3																		
	Break out (O)	Break out due to anthropogenic impact (aO)	Depth of aO in (cm) Intensity 1 < 0.5 Intensity 2 0.5 - 1.5 Intensity 3 > 1.5	1																		
				2																		
3																						
Break out due to constructional cause (bO)		Volume of bO in (cm ³ /m ²) [*] 1000 Intensity 1 < 2 Intensity 2 2 - 5 Intensity 3 5 - 10 Intensity 4 > 10	1																			
			2																			
			3																			
2- Discoloration (DD)	Loose salt deposits (E)	Efflorescence (Ee) Intensity 1 < 20 Intensity 2 20 - 50 Intensity 3 > 50	1																			
			2																			
Crust (C.)	Light colored crust tracing the surface (hkC)	Intensity of hkC Intensity 1 Low Intensity 2 Medium Intensity 3 High	1																			
			2																			
			3																			
3- Detachment of stone material (DT)	Granular disintegration (G)	Granular disintegration into sand (Gs) Intensity 1 < 2 Intensity 2 2 - 5 Intensity 3 5 - 10 Intensity 4 10 - 20 Intensity 5 > 20	1																			
			2																			
			3																			
			4																			
			5																			
4- Fissures / Deformation (FD)	Fissures (L)	Fissures dependent on stone structure (tL) Width of tL (cm) Intensity 1 < 0.5 Intensity 2 0.5 - 0.7 Intensity 3 0.7 - 1.0 Intensity 4 > 1.0	1																			
			2																			
			3																			
			4																			



Figure 8: Intensities of characteristic weathering forms at the selected parts at Seti I Temple

(Fig. 15). At higher magnification, micro-deformation of kaolinite texture and its splitting into loose sheets as well as K-feldspar that is traced at some parts of field view, halite is detected coating some parts of kaolinite and K-feldspar (Fig. 16).

4.2.2 Hydrochemical Results

Extracted solutions have been prepared from eleven rock samples (collected at the weathered parts of construction rock of Seti I Temple) and three soil samples (in contact with basal courses of this tem-

ple) following the method of [24]. The samples' number is limited as sampling from archaeological sites is restricted, but the collected samples are representative for each of the severely and slightly weathered parts of this temple. Eight samples (two from each part) of weathered sandstone (parts number 1, 2, 3 and 4, Fig. 1 b) and three samples of slightly weathered sandstone (representing parts number 5, 6, 7, 8 and 9, Fig. 1 b) have been collected. The electrical conductivity (E.C.), cations and anions (Ca⁺⁺, Mg⁺⁺, Na⁺, K⁺, Cl⁻, SO₄⁻⁻, CO₃⁻⁻,

Group	Main weathering forms	Individual weathering forms	Damage Categories and Intensities of the Individual weathering forms					
			Intensity class range	Damage Category (DCLS)	Intensity class range	Damage Category (DCLS)	Intensity class range	Damage Category (DCLS)
1- Loss of stone material (LS)	Back weathering (W)	(Wo)	Depth of Wo (cm)					
			Intensity class range	<0.5	0.5 ~ 0.8	0.8 ~ 1.3	1.3 ~ 2.0	> 2.0
			Damage Category (DCLS)	2	3	4	5	5
			Area % of total Wo					
			Intensity class range	< 5	5 ~ 20	20 ~ 25	25 ~ 40	> 40
			Damage Category (DCLS)	1	2	3	4	5
	Relief (R)	(Rh)	Depth of Rh (cm)					
			Intensity class range	< 1.5	1.5 ~ 2.5	> 2.5		
			Damage Category (DCLS)	3	4	5		
			Depth of aO (cm)					
	Break out (O)	(aO)	Intensity class range	<0.5	0.5 ~ 1.5	> 1.5		
			Damage Category (DCLS)	1	3	5		
			aO% of total area					
			Intensity class range	< 5	5 ~ 10	> 10		
Damage Category (DCLS)		1	2	3				
(bO)		Volume of bO (cm ³ /m ²) * 1000						
		Intensity class range	< 2	2 ~ 5	5 ~ 10	> 10		
		Damage Category (DCLS)	1	2	3	4		
	Ee% of total surface							
2- Discoloration (DD)	Loose salt deposits (E)	(Ee)	Intensity class range	< 20	20 ~ 50	> 50		
			Damage Category (DCDD)	1	2	3		
	Crust (C.)	(hkC)	Intensity of hkC					
			Intensity class range	Low	Moderate	High		
3- Detachment of stone material (DT)	Granular disintegration (G)	(Gs)	Mass of Gs (kg/m ²)					
			Intensity class range	< 2	2 ~ 5	5 ~ 10	10 ~ 20	< 20
			Damage Category (DCDT)	1	2	3	3	4
			Width of Fissure's aperture (cm)					
4- Fissures/ Deformation (FD)	Fissures (L)	(tL)	Intensity class range	< 0.5	0.5 ~ 0.7	0.7 ~ 1.0	> 1.0	
			Damage Category (DCFD)	2	3	4	5	

Figure 9: Correlation Scheme (Intensity classes - damage category) for the examined parts at Seti I Temple

HCO₃⁻) have been determined for these solutions using Ion Chromatograph supported by a computer system giving the concentration of these elements as part per million (ppm). Then, the type and percentage of the hypothetical dissolved salts have been computed using the hydrochemical equation; the results are listed in table 3.

Considerable difference can be noted in limits of electrical conductivity (E.C.) and total dissolved salts (T.D.S.) for the extracted solution of the collected sandstone samples. The slightly weathered sandstone has an electrical conductivity (E.C.) ranging from 9.6 to 12.8 mmhos/cm and total dissolved salts (T.D.S.) ranging from 18,904 to 23,735 ppm; the moderately weathered sandstone has an electrical conductivity 16.3 mmhos/cm and total dissolved salts 21,308 ppm; and that of the severely weathered

sandstone has E.C. ranging from 21.2 to 31.2 mmhos/cm and T.D.S. from 94,156 to 106,225 ppm. The dominant hypothetical dissolved salts in all sandstone samples are mostly chlorides (particularly NaCl salt) followed by sulphate salts (particularly Na₂SO₄ and low percentage of CaSO₄).

The soil samples have considerable E.C. ranging from 9.2 to 11.3 mmhos/cm and total dissolved salts ranging from 10,209 to 11,968 ppm with chlorides (particularly NaCl) as dominant hypothetical dissolved salts followed by sulphate (particularly Na₂SO₄ and CaSO₄) salts (Table 3).

4.2.3 Ultrasonic Waves Investigation

The ultrasonic waves' velocity and rock's internal friction (Cp and Qc respectively) are controlled by any variation in rocks' porosity either naturally

Table 2: Linear and progressive damage indices for the studied areas of Seti I Temple

Main weathering forms	Individual weathering forms	Part of investigation	Proportion of Damage Category %						DIlin	DIprog	Damage Index based on DI lin & DI prog	Average Damage Index based on DI lin & DI prog	Overall average damage index for each weathering form	
			Damage Category 0	Damage Category 1	Damage Category 2	Damage Category 3	Damage Category 4	Damage Category 5						
Back weathering (W)	Wo	1	0	0	5	25	70	0	3.65	3.69	4	4	5	4.1 i.e. Severe damage relevant to Wo
		2	0	0	5	30	65	0	3.60	3.65	4	4	5	
		3	0	0	0	25	70	5	3.80	3.83	4	4	5	
		4	0	0	5	30	65	0	3.60	3.65	4	4	5	
		5	0	0	10	65	25	0	3.15	3.20	3	3	4	
		6	0	0	0	50	45	5	3.55	3.60	4	4	5	
		7	0	10	25	60	5	0	2.60	2.70	3	3	4	
		8	0	20	55	25	0	0	2.05	2.16	2	2	2	
		9	0	25	50	25	0	0	2.00	2.12	2	2	2	
Relief (R.)	Rh	1	0	0	5	40	55	0	3.50	3.55	4	4	4	3.2 i.e. Moderate damage relevant to Rh
		2	0	0	5	45	50	0	3.45	3.50	4	4	4	
		3	0	0	10	35	50	5	3.50	3.58	4	4	4	
		4	0	0	15	30	55	0	3.40	3.48	4	4	4	
		5	0	10	5	55	30	0	3.05	3.17	3	3	3	
		6	0	5	5	45	45	0	3.30	3.39	3	3	3	
		7	0	15	20	60	5	0	2.55	2.67	3	3	3	
		8	0	15	55	30	0	0	2.15	2.25	2	2	2	
		9	0	25	50	25	0	0	2.00	2.12	2	2	2	
Break out (O)	(a.O)	1	60	40	0	0	0	0	0.40	0.63	0	1	1	1.4 i.e. very slight damage relevant to aO
		2	65	35	0	0	0	0	0.35	0.59	0	1	1	
		3	55	50	5	0	0	0	0.60	0.84	1	1	1	
		4	55	40	10	0	0	0	0.60	0.89	1	1	1	
		5	30	20	45	5	0	0	1.25	1.57	1	2	2	
		6	25	10	5	40	20	0	2.20	2.66	2	3	3	
		7	80	20	0	0	0	0	0.20	0.45	0	0	0	
		8	40	10	5	30	15	0	1.70	2.32	1	1	1	
		9	45	5	0	25	25	0	1.80	2.51	2	3	3	
	(b.O)	1	0	0	15	35	50	0	3.35	3.43	3	3	3	2.4 i.e. slight damage relevant to bO
		2	0	0	5	45	50	0	3.45	3.50	3	4	4	
		3	0	0	5	50	45	0	3.40	3.45	3	3	3	
		4	0	0	10	35	55	0	3.45	3.51	3	4	4	
		5	20	10	45	25	0	0	1.75	2.04	2	2	2	
		6	15	25	40	20	0	0	1.65	1.91	2	2	2	
		7	45	20	5	30	0	0	1.20	1.76	1	2	2	
		8	60	25	15	0	0	0	0.55	0.92	1	1	1	
		9	55	20	25	0	0	0	0.70	1.10	1	1	1	
Loose salt deposits (E)	(Ee)	1	5	10	5	15	50	15	3.40	3.66	3	4	4	2.67 i.e. Moderate damage relevant to Ee
		2	0	5	15	10	60	10	3.55	3.69	4	4	4	
		3	5	5	10	20	55	5	3.30	3.51	3	4	4	
		4	0	10	10	15	55	10	3.45	3.63	3	4	4	
		5	40	15	25	20	0	0	1.25	1.72	1	2	2	
		6	45	20	15	20	0	0	1.10	1.61	1	2	2	
		7	35	10	10	45	0	0	1.65	2.13	2	2	2	
		8	60	30	10	0	0	0	0.50	0.84	1	1	1	
		9	65	25	10	0	0	0	0.45	0.81	0	1	1	
Crust (C.)	(hkC)	1	40	20	30	10	0	0	1.10	1.52	1	2	2	1.67 i.e. Slight damage relevant to hkC
		2	35	30	35	0	0	0	1.00	1.30	1	2	2	
		3	45	35	20	0	0	0	0.75	1.07	1	1	1	
		4	40	30	30	0	0	0	0.90	1.22	1	1	1	
		5	55	40	5	0	0	0	0.50	0.77	1	1	1	
		6	50	35	15	0	0	0	0.65	0.97	2	2	2	
		7	45	30	25	0	0	0	0.80	1.14	2	2	2	
		8	50	40	10	0	0	0	0.60	0.89	2	2	2	
		9	55	30	15	0	0	0	0.60	0.95	2	2	2	
Granular disintegration (G)	(Gs)	1	0	5	10	40	45	0	3.25	3.35	3	3	4	3.78 i.e. Severe damage relevant to Gs
		2	0	10	5	40	45	0	3.20	3.33	3	3	4	
		3	0	0	5	20	50	25	3.95	4.03	4	4	5	
		4	0	0	10	20	55	15	3.75	3.84	4	4	5	
		5	3	5	10	30	50	2	3.25	3.41	3	3	4	
		6	0	5	15	15	60	5	3.45	3.58	3	4	4	
		7	5	10	20	45	15	5	2.70	2.93	3	3	4	
		8	35	30	20	15	0	0	1.15	1.57	1	2	2	
		9	40	30	15	15	0	0	1.05	1.50	1	2	2	
Fissures (L)	(tL)	1	5	5	10	55	25	0	2.90	3.07	3	3	4	2.33 i.e. Slight damage relevant to tL
		2	5	10	10	50	25	0	2.80	3.00	3	3	4	
		3	5	5	25	50	15	0	2.65	2.82	3	3	4	
		4	10	5	20	55	10	0	2.50	2.72	3	3	4	
		5	40	30	30	0	0	0	0.90	1.22	1	1	1	
		6	35	30	35	0	0	0	1.00	1.30	1	1	1	
		7	45	40	15	0	0	0	0.70	1.00	1	1	1	
		8	60	40	0	0	0	0	0.40	0.63	0	1	1	
		9	65	35	0	0	0	0	0.35	0.59	0	1	1	

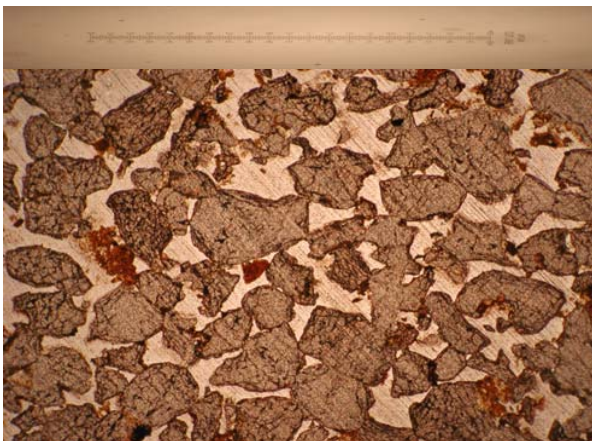
(change of homogeneity due to textural changes or variation along direction in the same sample of laminated rocks as well as due to natural weathering) or artificially (on artificial weathering) [14, 22]. The velocity of ultrasonic waves is increased and rock's internal friction is decreased as rock has better physical nature (less weathered and highly compact rock). Hence, ultrasonic waves' investigation as a non-destructive technique has been con-

ducted for eight rock samples: two samples from part 1 having medium size light brown quartz arenite and two samples of same type from each of parts 3, 5 and 9. This medium size light brown sandstone is selected for such investigation as it dominates as construction rock of this temple, it is very similar to sandstone type 1 of El-silsila quarries, the results are listed in table 4.

		DCDD												DCDT	
		0			1			2			3				
		4	4	5	4	4	5	4	4	5	4	4	5		
DCLS	0	4	4	5	4	4	5	4	4	5	4	4	5	4	
		3	3	4	3	3	4	3	3	4	3	3	4	3	
		2	2	3	2	2	3	2	2	3	3	3	3	3	
		1	2	3	2	2	3	2	2	3	3	3	3	3	
	1	0	2	3	2	2	3	2	2	3	3	3	3	3	
		4	4	5	4	4	5	4	4	5	4	4	5	4	
		3	3	4	3	3	4	3	3	4	3	3	4	3	
		2	2	3	2	2	3	2	2	3	3	3	3	3	
	2	1	2	3	2	2	3	2	2	3	3	3	3	3	
		1	2	3	2	2	3	2	2	3	3	3	3	3	
		4	4	5	4	4	5	4	4	5	4	4	5	4	
		3	3	4	3	3	4	3	3	4	3	3	4	3	
	3	2	3	3	3	3	3	2	3	3	3	3	3	3	
		2	2	3	2	2	3	2	2	3	3	3	3	3	
		2	2	3	2	2	3	2	2	3	3	3	3	3	
		5	5	5	5	5	5	5	5	5	5	5	5	5	
	4	4	4	5	4	4	5	4	4	5	4	4	5	4	
		3	3	4	3	3	4	3	3	4	3	3	4	3	
		3	3	4	3	3	4	3	3	4	3	3	4	3	
		3	3	4	3	3	4	3	3	4	3	3	4	3	
5	5	5	5	5	5	5	5	5	5	5	5	5	5		
	5	5	5	5	5	5	5	5	5	5	5	5	5		
	4	4	5	4	4	5	4	4	5	4	4	5	4		
	4	4	5	4	4	5	4	4	5	4	4	5	4		
5	4	4	5	4	4	5	4	4	5	4	4	5	4		
	4	4	5	4	4	5	4	4	5	4	4	5	4		
	5	5	5	5	5	5	5	5	5	5	5	5	5		
	5	5	5	5	5	5	5	5	5	5	5	5	5		
		0	2	3	0	2	3	0	2	3	0	2	3		
DCFD															

- DCLS - Damage categories for all weathering forms of group 1 "Loss of stone material"
- DCDD - Damage categories for all weathering forms of group 2 "Discoloration/ deposits"
- DCDT - Damage categories for all weathering forms of group 3 "Detachment"
- DCFD - Damage categories for all weathering forms of group 4 "Fissures/ deformation"

Figure 10: Scheme for the determination of damage categories considering all groups of weathering forms "DCAW", Seti I Temple



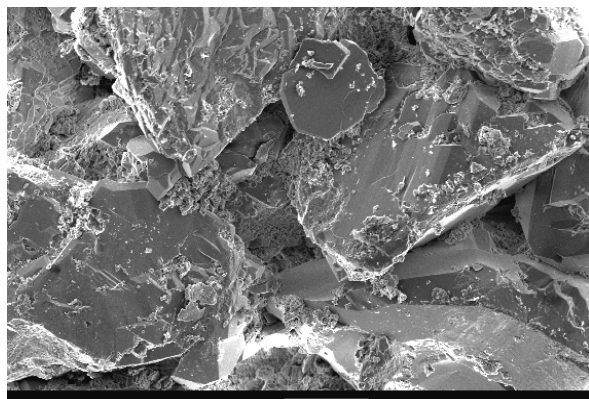
S.S. (40x mag., plane polarized light)

Figure 11: Thin section photo-micrograph presenting rock texture of medium size sandstone of Seti I Temple.



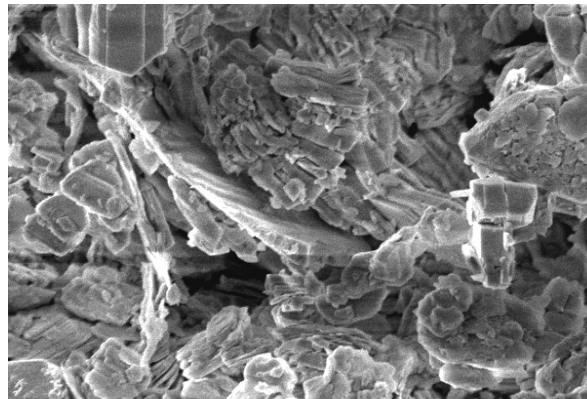
S.S. (40x mag., plane polarized light)

Figure 12: Thin section photo-micrograph presenting rock texture of fine grained sandstone of Seti I Temple.



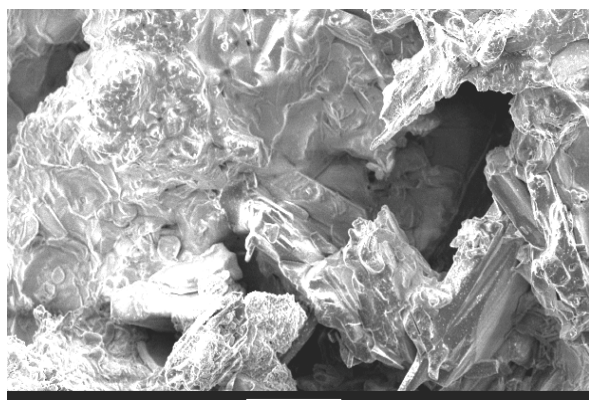
330 x mag 50 microns

Figure 13: Scanning electron photo-micrograph presenting micro-fragmentation of silica overgrowth, iron oxide within rock pores.



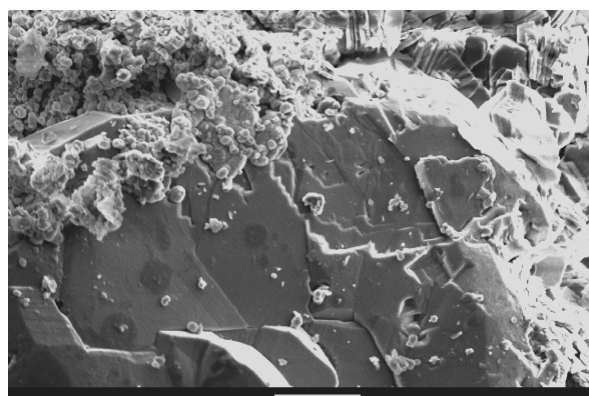
6k mag. 5 microns

Figure 16: Scanning electron photo-micrograph presenting deformation in Kaolinite and feldspar texture by salt crystals, sandstone of Seti I Temple.



400x mag 50 microns

Figure 14: Scanning electron photo-micrograph presenting Halite coating most of the sandstone components, Seti I Temple.



1700x 10 microns

Figure 15: Scanning electron photo-micrograph presenting fragmentation of silica overgrowth and pitting; Kaolinite and ball shape iron oxide within pores of construction sandstone.

The difference in ultrasonic waves' velocity "Cp" and rock's internal friction "Qc" for the various parts of Seti I Temple is a reflection of its relative weathering intensity to each other on one hand (Table 4) and to the fresh (un-weathered) equivalent type 1 of Gebel El-Silsila on the other hand (Table 5). The rock's limit of an-isotropy index (computed by dividing Cp measured parallel to bedding by Cp measured at right angle to bedding planes) of the examined rock samples compared with un-weathered similar rock (collected from El-Silsila quarries) also reflects relative weathering intensity. Such weathering resulted in weakness and deformation of rock's internal texture at a preferred orientation (parallel to bedding), thus, its an-isotropy index is increased (Table 4).

5 Discussion

For the first step in quantifying damage category of Seti I Temple, field investigation included recording all weathering forms and its dimensions at each part of the Seti I Temple as presented in table 1 and figure 8. The damage category over each wall side can be defined based on the frequency and type of each weathering form where frequent obliteration of engravings and/or exfoliation means high damage category, but frequent pitting at non-engraved stone might indicate low damage category. The damage category is not only controlled by stone type (that is sandstone all over Seti I Temple) and its properties [25, 26] but also on wall side orientation that controls number, duration and intensity of weathering cycles [25, 27-31]. It is found that wall sides under investigation at Seti I

Table 3: Hydrochemical analysis for extracted solutions prepared from rock samples collected from Seti I Temple and soil samples at the same temple

Sample number	Part number at Seti I Temple	Sample type and state	E.C. (mmhos/cm)	T.D.S. (ppm)	Cations (ppm)				Anions (ppm)				Hypothetical Dissolved Salts %							
					Ca++	Mg++	Na+	K+	Cl-	SO4--	CO3--	HCO3-	KCl	NaCl	Na2SO4	CaSO4	MgSO4	CaCO3	MgCO3	Mg(HCO3)2
1	1	W.S.S.	31,2	103156	2235	370	56270	1760	30810	11650	0	61	1,7	76,3	16,4	4,3	1,2	0	0	0
2	1	W.S.S.	30,9	100040	2045	420	50178	2110	35249	9640	187	211	2,3	80,7	11,1	4,4	1,2	0	0,3	0
3	2	W.S.S.	28,7	94156	2167	210	49983	1659	27654	12170	94	219	1,9	73,1	19,6	4,4	0	0,3	0	0,7
4	2	W.S.S.	21,2	96361	1996	527	51234	1894	29870	10598	115	127	2	78,8	13	4,1	0	0	1,6	0,5
5	3	W.S.S.	27,1	106225	2170	276	60324	875	32569	9834	60	117	0,8	80,2	14,1	3,9	0	0,1	0,3	0,5
6	3	W.S.S.	29,3	102895	1870	449	56894	935	30976	11450	111	210	0,9	77,1	16,9	3,6	0,5	0	0,4	0,6
7	4	W.S.S.	30	101359	1976	325	58964	769	28765	10560	0	0	0,7	78,3	16,2	3,7	1,1	0	0	0
8	4	W.S.S.	26,9	99910	2015	298	51234	937	33986	11440	0	0	1	79	14,6	4,3	1,1	0	0	0
9	5	S.W.S.S.	12,8	23735	1210	230	8873	116	8743	4563	0	0	0,6	71,4	1,6	13,1	3,3	0	0	0
10	7	M.W.S.S.	16,3	21308	987	179	7970	154	6798	5220	0	0	1	63	20,3	12,1	3,6	0	0	0
11	8	S.W.S.S.	9,6	18904	1120	210	5859	256	7670	3789	0	0	2	71	4,7	17	5,3	0	0	0
12	SOIL 1	SOIL 1	10,1	10209	870	83	4320	76	3210	1650	0	0	0,8	71,2	6,6	18,4	3	0	0	0
13	SOIL 2	SOIL 2	9,2	11968	610	76	6720	102	2765	1599	0	96	0,8	68,2	19,7	9,4	0,9	0	0	1
14	SOIL 3	SOIL 3	11,3	11530	766	91	5433	154	3099	1987	0	0	1,4	66,6	15,7	13,6	2,7	0	0	0

N.B. S.W.S.S. is slightly weathered sandstone sample
M.W.S.S. is moderately weathered sandstone sample
W.S.S. is severely weathered sandstone sample

Table 4: Velocity of ultrasonic waves and rock's internal friction of Seti I Temple's construction rock

Part number of sample collection	Sample number	Ultrasonic Parameters			
		Cp (km/sec)		Anisotropy index (Cp1/Cp2)	Internal friction "Qc"
		Parallel to bedding (Cp1)	at right angle to bedding (Cp2)		
1	1	1,53	1,38	1,11	8,1
1	2	1,58	1,40	1,13	8,3
3	3	1,50	1,37	1,09	8,4
3	4	1,55	1,40	1,11	8,0
5	5	1,99	1,89	1,05	7,0
5	6	1,92	1,87	1,03	6,5
9	7	2,01	1,93	1,04	6,2
9	8	2,00	1,91	1,05	6,3

Table 5: Limits of physical parameters of sandstone type one of El-Silsila quarries at different states (Kamh, 2007)

Sandstone type 1	Ultrasonic Parameters		
	Cp parallel to bedding (km/sec)	Cp at right angle to bedding (km/sec)	Rock's internal friction "Qc"
Un-weathered	2,14	2,32	6,6
5 cycles of soundness test using 14% NaCl solution	2,18	2	6,9
10 cycles of soundness test using 14% NaCl solution	1,9	1,71	7,4
15 cycles of soundness test using 14% NaCl solution	1,67	1,55	7,91

Temple can be arranged from high damage category to low damage category wall side as follows: East facing wall side then West and South facing wall sides respectively. The East facing wall side receives longer time of solar heating enabling severe drying of damp-salty construction rock, hence, salt crystallization (of chloride salts, Table, 3 and Figs. 14 and 16) takes place destroying rock's texture on both micro and mega-scale than other wall sides. The damage on microscale is reported particularly for minerals with cleavage as K-feldspar and flaky Kaolinite (Fig. 16).

The correlation scheme (Fig. 9) is a clear and strong presentation of damage category and intensity class that is based on dimensions (e.g. area percentage affected by the weathering form, depth or thickness of stone surface removed by weathering form, rock volume detached from the blocks) of each weathering form. For example, a weathering feature as obliteration of engravings (W_o) represent a damage category 5 (very severe category) for the wall side or the whole site if it covers more than 40 % of the total engraved surface area. This is because W_o is a very effective weathering form as it directly attach rock's engravings that give the stone a historical value. The mathematical computing of damage category (at the present time DI_{in}) at each part of Seti I Temple and the expected damage in the future (DI_{prog}) enable finding out to which limit of damage does the site is going to. This is sort of quantifying damage category at this temple based on the accurate field measurements and this is useful particularly at sites where sampling is impermissible.

All result in a conclusion that damage category at some parts of Seti I Temple reaches up to severe and very severe damage (as areas including parts number 1, 2, 3 and 4 regarding granular disintegration that ends by obliteration of engravings and clearing out of stone components, table 2) and down to slight and very slight damage category (as areas including parts number 5, 6, 7, 8 and 9 regarding break out and fissures, table 2). The overall damage category for this temple based on field investigation considering all weathering forms is found to be very severe damage category (Fig. 10).

The laboratory investigations have been conducted to reflect an image for rock's texture, weathering detection on micro-scale on one hand and to numerically quantify rock's salt content and its geotechnical properties' limit. All enable quantitative definition of rock's damage category for that monumental sandstone at this arid region.

The laboratory investigations revealed similarity of construction rock (in its texture and composition) to sandstone (type 1) of El-Silsila quarries that verified to be relatively durable sandstone compared with other sandstone types of this huge quarry [17]. The rock's texture is mature but still has kaolinite and K-feldspar that show deformation on micro-scale by salt crystallization (Halite that has been detected using SEM and hydrochemical analysis) at such arid to extremely arid climate. At super-saturated salt solutions within rock pores, halite is expected to

crystallize in a Whiskers form that was reported to exert severe pressure on rock's pores deforming most of rock types [32 - 34].

The total dissolved salts at the examined parts of Seti I Temple indicated that some parts have considerably high total dissolved salts (reaching up to 106,225 ppm) compared with the Islamic archaeological sites in Cairo that are flooded with domestic water and suffer severe salt weathering (at arid climate) with T.D.S. reaching up to 142,000 ppm [35]. The near surface groundwater is raised with its dissolved salts by capillary force within the lower courses of Seti I Temple up to heights of 2 m above ground surface, then moves horizontally to reach stone surface, water evaporates at such arid climate leaving salts at and on stone surface deforming rock's texture on salt crystallization particularly for chloride salts.

The recession in limits of geotechnical parameters for the same rock at the examined parts of the temple quantifies weathering intensity at these parts relative to each other and relative to El-Silsila un-weathered sandstone (type 1). Comparing limits of geotechnical parameters (measured using ultrasonic waves) of the naturally weathered sandstone type one of Seti I Temple (Table 4) with that of fresh and artificially weathered sandstone of El-Silsila quarries (Table 5), it can be noted that the parts of investigation number 1 and 3 have lower limits of C_p than limits of El-Silsila sandstone (at its un-weathered state and after 15 cycles of intensive artificial weathering). This means that at such parts, the damage is severe in its intensity. Investigation parts number 5 and 9 have limits of C_p and Q_c very close to limits of El-Silsila sandstone type one after its exposure to 5 cycles of soundness test i.e. it is parts with slight damage category. Comparing the semi-quantitative determination of damage category (through field investigations and its data processing, Table 2 and Fig. 10) with the quantitative evaluation defined by laboratory measurements (for samples geotechnical properties, Tables 4 and 5), great compatibility can be noted between them confirming the validity of using field investigations to define damage category for a given monumental site. Also, from the field investigations and laboratory analyses, it is noted that the whole temple has a very severe damage category, consequently, it requires urgent plan of restoration particularly for the parts of investigation numbers 1, 2, 3 and 4.

6 Conclusions

Detailed field investigations involving measuring dimensions of weathering forms, using damage category scale and computing linear and progressive damage indices enable semi-quantifying of damage category at the selected parts (representing all weathering forms and damage grades) at Seti I Temple. It revealed that this site has severe to very severe damage category regarding obliteration of engravings and granular disintegration weathering forms, but slight to very slight damage category regarding most of the other weathering forms. The whole site has very severe damage category.

Laboratory investigations have been conducted to quantify damage category for such construction rock relative to each other and relative to its un-weathered El-Silsila sandstone quarries. The results indicated that it is quartz arenite to arkosic sandstone similar to sandstone type 1 of El-Silsila quarries (light brown spotted sandstone), has considerable salt content (particularly at the basal courses) ranging from 18,904 ppm up to 106,225 ppm (mainly NaCl, Na₂SO₄ and CaSO₄ salts). Such salts result in deformation (on micro-scale) of labile minerals particularly K-feldspar and kaolinite constituting this rock. The recession in velocity of ultrasonic waves "Cp" and the increase in rock's internal friction "Qc" reflects damage category particularly on comparing highly damaged parts with the moderately or slightly damaged parts on one hand, and on comparing weathered parts with the un-weathered and the artificially weathered sandstone of El-Silsila quarries. The quantitative laboratory investigations revealed an overall severe recession in limits of geotechnical parameters of Seti I Temple's construction rock. These laboratory investigations confirm that the semi-quantitative definition of the overall damage category conducted through detailed field study for this site can safely replace the detailed laboratory techniques that are based on sampling from such archaeological sites that is mostly impermissible.

Acknowledgement

The authors express their deep thanks to Lehrstuhl for Engineering Geology und Hydrogeology, particularly to Dr. M. Lambarki as well as to Geophysics Dept. particularly to Dr. Klitzsch at Aachen University (RWTH), Germany for conducting laboratory work of this research.

References

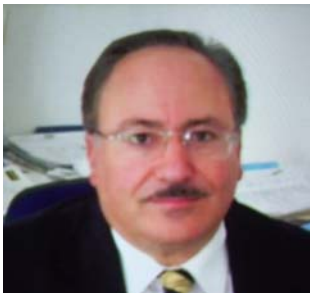
1. A. Dragowski; R. Kaczynski and J. Wroblewski, *Engineering geological problems related to the reconstruction of the Hatshepsut Temple in Deir El-Bahari*, Engineering Geology of ancient works, monuments and historical sites, Marinis and Koukis "eds", **1**, 161 – 168 (1988).
2. L. Angel; A. Maria and O. Salvador, *The physico-chemical weathering of monumental dolostone, granites and limestones; dimension stones of the Cathedral of Toledo (Spain)*, J. Stone, **11**, 197 – 215 (1994).
3. B. M. Ismail, *Study of the deterioration phenomena in the Ptolemaic Temple of Dendara, Egypt*, Bull. of the Fac. of Eng., Assiut Univ., **27 (1)**, 20 – 27 (1999).
4. M. Montoto; L. Valdeon; P. Cotte; L. Calleja and R. M. Esbert, *Non-destructive characterization of the state of deterioration of Megaliths by ultrasonic tomography: a petrophysical interpretation*, Proc. of 9th Int. Congress on Deterioration and Conservation of Stone, Amsterdam, Elsevier, 3 – 9 (2000).
5. G. M. E. Kamh and H. Hanna, *Measuring rock surface roughness by micro-erosion meter as indication of weathering of St. John Medieval Church, Chester City, UK*, Egyptian Journal of Geology, **46 (2)**, 461 – 469 (2002 a).
6. G. M. E. Kamh and H. Hanna, *Weathering processes of St. John Church with an emphasis on salt weathering, Chester City, UK*, Bull. Fac. of Sci., Assiut Univ., **31 (2-F)**, 151 – 163 (2002 b).
7. B. Fitzner; K. Heinrichs and D. La Bouchardiere, *Weathering damage on pharaonic sandstone monuments in Luxor, Egypt*, Building and Environment, **38**, 1089 – 1103 (2003).
8. G. M. E. Kamh, *The impact of windblown and bedrock un-stability on Greco-Roman archaeological sites at Kom Oshim, El-Fayum Province, Egypt*, Annals of the Geological Survey of Egypt, **25**, 535 – 548 (2002).
9. G. M. E. Kamh, *Geological study and weathering processes on archaeological sites at humid regions – Hilltop Beeston Castle, Great Britain, a case study*, Int. J. for Restoration, **10 (3)**, 251 – 274 (2004).
10. A. H. Webb; R. J. Bawden; A. K. Busby and J. N. Hopkins, *Studies on the effects of air*

- pollution on limestone degradation in Great Britain*, Atmospheric Environment, **26 B (2)**, 165 – 181 (1992).
11. F. Guidobaldo and A.M. Mecchi, *Corrosion of ancient marble monuments by rain: evaluation of pre-industrial recession rates by laboratory simulations*, Atmospheric Environment, **27 B(3)**, 339 – 351 (1993).
 12. A. G. Nord; A. Svårdh and K. Tronner, *Air pollution levels reflected in deposits on building stone*, Atmospheric Environment, **28 (16)**, 2615 – 2622 (1994).
 13. M. S. Vendrell; M. Garcia and S. Alarcon, *Environmental impact on the Roman monuments of Tarragona, Spain*, Environmental Geology, **27**, 263 – 269 (1996).
 14. S. Simon and A. M. Lind, *Decay of limestone blocks in the block fields of Karnak Temple (Egypt): Non-destructive damage analysis and control of consolidation treatments*, J. Stone, **14**, 743 – 749 (2000).
 15. K. Zehender; A. Arnold and K. Andreas, *Weathering of painted marly limestone in the temple ruin of Merenptah, Qurna- Luxor, Egypt*, 9th Int. Congress on Deterioration and Conservation of Stone, Venice, June 2000, 749 – 757 (2000).
 16. B. Fitzner; K. Heinrichs and D. La Bouchardiere, *Damage index for stone monuments. Protection and Conservation of the Cultural Heritage of the Mediterranean Cities*, Proceedings of the 5th Int. Symposium on the Conservation of Monuments in the Mediterranean Basin, Sevilla, Spain, 5-8 April 2002: 315 – 326 (2002).
 17. G. M. E. Kamh, *Petrographic, geotechnical and durability investigations for the Upper Cretaceous Nubian sandstone quarries used for restoration, Upper Egypt, case study*, International Journal for Restoration of Buildings and Monuments, **13 (1)**, 39 – 56 (2007).
 18. R. A. J. Wüst, *The origin of soluble salts in rocks of the Thebes Mountains, Egypt: The damage potential to ancient Egyptian wall art*, Journal of Archaeological Science, **27**, 1161 – 1172 (2000).
 19. G. M. E. Kamh, *The impact of landslide and salt weathering on Roman structures at high latitudes- Conway Castle, Great Britain: a case study*, Int. Journal of Geosciences “Environmental Geology”, **48 (2)**, 238 – 254 (2005).
 20. R. Said, *The Geology of Egypt*. Rotterdam: Balkema, 734 (1990).
 21. G. Kirchner, *Cavernous weathering in the Basin and Range area, South-western USA and North-western Mexico*, Z. Geomorph. N. F., **106**, 73 – 97 (1996).
 22. G. M. E. Kamh, *Evaluation of seven resins as stone surface consolidants for four limestone facies using a magneto-structive ultrasonic technique*, Int. J. for Restoration of Buildings and Monuments, **9 (2)**, 149 – 172 (2003).
 23. P. A. Kapranos; M. H. H. Al-Helaly and V. N. Whittaker, *Ultrasonic velocity measurements in 316 Austenitic Weldments*, British Journal of non-destructive testing, **23 (6)**, 211 – 222 (1981).
 24. J. D. Rhoades, “Soluble salts”, *Methods of soil analysis, part 2: Chemical and microbiological properties*, Agronomy Monograph No. 9 (2nd edition) (1982).
 25. D. McCarroll and A. Nesje, *Rock surface roughness as an indicator of degree of rock surface weathering*, Earth Surface Processes and Landforms, **21**, 963 – 977 (1996).
 26. Y. Matsukura and N. Matsuoka, *The effect of rock properties on rates of tafoni growth in coastal environments*, Z. Geomorph. N. F., **106**, 57 – 72 (1996).
 27. M. Montoto; L. Callega; B. Perez and R. M. Esbert, *Evaluation in Situ of deterioration of monumental stones by non-destructive ultrasonic techniques*, Mat. Res. Soc. Symp. Proc., **185**, 273 – 284 (1981).
 28. D. N. Mottershead, *Coastal spray weathering of bedrock in the supratidal zone at East-Prawle, South Devon*, Field Studies, **5**, 663 – 684 (1981).
 29. M. Bennett, *A simple physical model of dry deposition to a rough surface*, Atmospheric Environment, **22 (12)**, 2701 – 2705 (1988).
 30. R. S. Prakasa; L. T. Khemani; G. A. Momin; P. D. Safai and A. G. Phillai, *Measurements of wet and dry deposition at an urban location in India*, Atmospheric Environment, **26B (1)**, 73 – 78 (1992).
 31. G. D. Hoke and D. L. Turcotte, *The weathering of stones due to dissolution*, Environmental Geology, **7**, 254 – 270 (2004).
 32. C. A. Moses and B. J. Smith, *Limestone weathering in the supra-tidal zone: An example from Mallorca*. Rock Weathering

- and Landform Evolution, Robinson and Williams "eds", 433 – 451 (1994).
33. N. S. Theodore and B. Nicholas, *Inversion of marble sulfation - reconversion of gypsum films into calcite on the surfaces of monuments and status*. Studies in Conservation, **29**, 197 – 204 (1994).
34. A. V. Turkington, *Gypsum formation in non-calcareous building sandstone: a case study of Scrabo Sandstone*, Earth Surface Processes and Landforms, **26**, 869 – 875 (2001).
35. G. M. E. Kamh, *The impact of geological conditions on the Islamic archaeological sites at El-Gammalia area, Cairo City, Egypt*, M.Sc. Thesis, Fac. of Sci., Menoufiya University (1994).



Dr. Gamal Mohamed Esawy Kamh obtained first a BSc and a MSc in Geology. He obtained a PhD in 2000 with a thesis entitled "A comparative study on the impact of environmental geological conditions on some archeological sites at Giza (Saqara region) and Alexandria Governorates and their modes of preservation". At present he holds the position of an Associated Professor in the Geology Department, Faculty of Science, Menoufiya University, Egypt.
E-mail: g_kamh2000@yahoo.com



Professor Dr. Rafiq Azzam is professor of engineering geology and currently works as head of Engineering Geology and Hydrogeology Department, RWTH, Aachen University, Germany.

Received July 19, 2007